Quantitative Evaluation of Automated Robot-Assisted Volumetric Breast Ultrasound

Anton V. Nikolaev
Department of Radiology, Nuclear Medicine and Anatomy
Radboud UMC
Nijmegen, the Netherlands
https://orcid.org/0000-0002-5522-9238

Leon de Jong
Department of Radiology, Nuclear Medicine and Anatomy
Radboud UMC
Nijmegen, the Netherlands
leon.dejong@radboudumc.nl

Vincent Groenhuis
Robotics and Mechatronics
University of Twente
Enschede, the Netherlands
v.groenhuis@gmail.com

Marcel K. Welleweerd
Robotics and Mechatronics
University of Twente
Enschede, the Netherlands
m.k.welleweerd@utwente.n

Françoise J. Siepel
Robotics and Mechatronics
University of Twente
Enschede, the Netherlands
f.j.siepel@utwente.nl

Stefano Stramigioli,
Robotics and Mechatronics
University of Twente
Enschede, the Netherlands
s.stramigioli@utwente.nl

Hendrik H. G. Hansen
Department of Radiology, Nuclear Medicine and Anatomy
Radboud UMC
Nijmegen, the Netherlands
rik.hansen@radboudumc.nl

Chris L. de Korte
Department of Radiology, Nuclear Medicine and Anatomy
Radboud UMC
Nijmegen, the Netherlands
chris.dekorte@radboudumc.nl

Abstract— **Adding volumetric ultrasound (3DUS) to MRI improves cancer detection rate in a breast. However, the fusion of 3DUS and MRI is challenging due to the different position (supine versus prone, respectively) and high deformation of a breast in the existing 3DUS scanners. In this study, we present and quantitatively evaluate a novel robot-assisted breast scanning system for 3D US acquisitions. Since the breast is scanned in a prone position with minimal and measurable deformation, this can facilitate MRI – 3DUS fusion.**

For quantitative evaluation, a breast-shaped rigid polyvinyl-alcohol phantom was constructed containing spherical lesions (15 mm diameter) with different echogenicity (-22 dB, -5 dB, -4 dB, 3 dB, 7 dB).

First, the phantom was scanned with a Siemens Skyra 3T MRI (Siemens Healthcare, Erlangen, Germany). Next, the phantom was scanned by a robotic arm (KUKA, Augsburg, Germany) (Fig.1a.) following a pre-planned spiral trajectory, determined from the MRI volume. The flange of the robot was equipped with an L10-5v US transducer attached to a P500 system (Siemens, Mountain View, CA, US). 2D B-mode US data were acquired for 3 minutes at 12 fps. The imaging depth was 5 cm, and the focal depth was set at 2 cm.

A volume of 77 x 77 x 69 mm3 was reconstructed with an isotropic sampling distance of 0.2 mm utilizing a voxel nearest neighbor method with a subsequent "hole filling" step, i.e. interpolation. The contrast-to-noise ratio (CNR) and signal-to-noise ratio (SNR) were calculated per lesion and compared to reference values from the originally acquired 2D B-mode images.

The 3D US volume was registered to the MRI volume by using 4 lesions as landmark, using rigid registration. The distance between the centers of the remaining lesion in MRI and 3DUS after the registration was calculated. The measurement was repeated for 5 combinations between lesions and landmarks. The average distance was used as a measure of registration accuracy.

For the reconstructed volume only 24% of the data were obtained by interpolation. On average, the CNR and SNR were 24% and 6% higher, respectively, for the 3DUS compared to the reference. The registration accuracy was 3.4 mm; hence, the presented scanning approach enables ultrasound breast 3D imaging in prone position facilitating MRI – 3D US fusion.

Keywords—quantitative analysis, MRI and US registration, robotic assisted US imaging, breast biopsy, breast phantom

I. Introduction

One out of 7 women will get breast cancer, and in 11 countries of the world, it is even the most frequent cause of death [1]. Early and reliable diagnosis is of paramount importance for the timely treatment of breast cancer since early diagnosis reduces mortality and morbidity [2]. Currently, ultrasound-guided Core Needle Biopsy (CNB) is the preferred technique to determine lesion malignancy. However, CNB strongly depends on the operator and in some cases results in false-negative diagnosis [3]. In addition, in case of US occult lesions US-guided CNB is not applicable and a more complex MRI-guided biopsy is performed instead. Robotic-assisted ultrasound-guided biopsy is a modern technology, aimed to overcome abovementioned drawbacks of CNB in an operator- independent way. Similar to conventional CNB, the robot images the region of interest (ROI) to localize the target. Next, after the position of the target is identified, the needle can be inserted [4]. Nevertheless, this technology is still not applicable to US occult lesions.

The MRI and US Robotic Assisted breast Biopsy system (MURAB) [5] is a novel technology that combines flexibility of US and sensitivity of MRI. Similar to MRI, the system performs 3D ultrasound imaging of a breast while the patient is in a prone position. The target lesions are localized by registering the 3D US volume to pre-MRI data, acquired in advance. Hence, this technology is also applicable for US occult lesions

978-1-7281-5448-0/20/$31.00 ©2020 IEEE

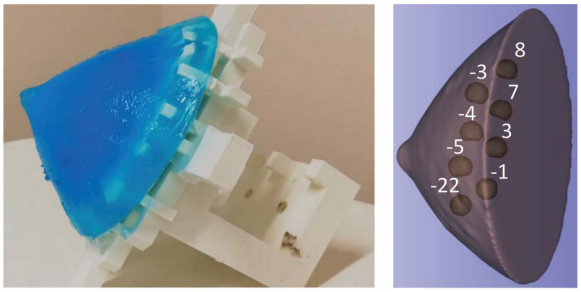

(a) (b)

Fig. 1. (a) Fabricated QBP. (b) MRI data of QBP with internal structure visible.

Since 3D US imaging is a crucial step of the MURAB technology, this paper is focused on quantitative evaluation of the automated robot-assisted volumetric breast ultrasound. In this work we assess the image quality of the resulting 3D US data and the registration accuracy with MRI.

II. Materials and Methods

A. Quantitative Breast Phantom

A stiff custom-made Quantitative Breast Phantom (QBP) was designed and fabricated for quantitative evaluation of the result volumetric US images(Fig. 1). The QBP was made by freeze-thawing 10% out of Polyvinyl Alcohol (PVA) solution and contained 8 spherical lesions of different echogenicity (8 dB, 7 dB, 3 dB, -1 dB, -3 dB, -4 dB, -5 dB, -22 dB). The diameter of each lesion was 15 mm.

B. System Design

The system was based on aKUKA robotic arm (KUKA, Augsburg, Germany). An end-effector [6] was attached to the flange of the robotic arm and comprised an L10-5v US transducer (Siemens, Mountain View, CA, US) and an optical stereo camera as depicted in fig 2. The US transducer was connected a Siemens P500 US imaging system (Siemens, Mountain View, CA, US). The system is operated via a control PC. Post-processed B-mode images were captured by the PC with a video grabber. Simultaneously the transformation matrices of the flange of the robotic arm were saved.

C. Data Acquisition Workflow

The volumetric imaging workflow consists of 3 basic steps: 1) pre – MRI acquisition, 2) scanning trajectory planning and localization, and 3) ultrasound scanning.

The pre-MRI acquisition was performed one day before the ultrasound acquisitions with a Siemens Skyra 3T MRI (Siemens Healthcare, Erlangen, Germany). Scanning trajectory planning and localization is a complex procedure based on the pre-MRI data which will be described next. It has to be carried out right before the US imaging.

The trajectory was made by projecting a spiral line on the surface of the breast observed in the MRI data. To approximately localize the trajectory in the coordinate system of the robot, first the robotic arm, first, moves around the QBP to capture the optical images with the stereo camera. Next, the acquired optical data are registered to the MRI volume.

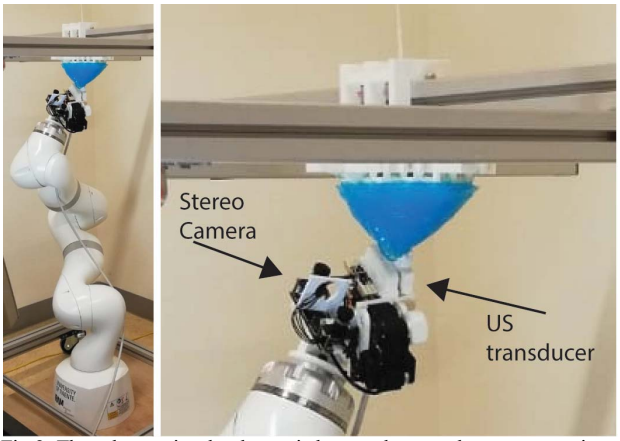

Fig 2. The robot-assisted volumetric breast ultrasound system overview.

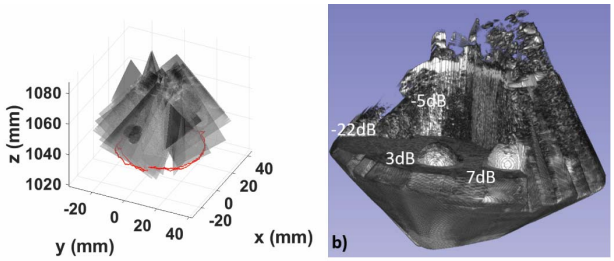

(a) (b)

Fig. 3. (a) Spatially combined B-mode images after applying formula 1. (b) Rendered 3D US data.

Then, during the ultrasound scan, the robotic arm follows the pre-planned trajectory, trying to keep a contact force of ~4N between the transducer and the QBP. The robot moves around the QBP at a speed of 2 mm/s resulting in a 3-minute scan for the full trajectory. The US acquisition was done with 12fps with a penetration depth of 5cm and a focal distance of 2cm.

D. Pre-processing

Before reconstruction, attenuation correction was applied to each B-mode US image. Furthermore, on each image, the 'blind areas', *i.e.* the areas without contact with the phantoms surface, was detected and excluded as described in [7]. Temporal calibration was performed by compensating the time delay between image and coordinate frames by:

$$p^{i,j} = H^{i-\Delta^w_f} \cdot H^{i-\Delta^f_t} \cdot p_0^{i,j}, \qquad (1)$$

where i is the index of the current image, j is the number of a certain pixel, p, within the i^{th} image, Δ is a time delay expressed in frames, H_f^w is a transformation matrix from the flange to the world coordinate system, H_t^f is a transformation matrix from the transducer to flange coordinate system. The algorithm was implemented in Matlab 2019 (MathWorks, Natick, USA).

Spatial calibration was not required since the transformation between the transducer's surface and the flange was known from the design of the end-effector [8].

E. Volumetric Reconstruction

The volume was reconstructed by transforming all acquired data into a point cloud utilizing equation 1 first. Next, using the Voxel Nearest Neighbor method (VNN) with a subsequent 'hole filling' step, i.e. interpolation, the point cloud was transformed into the volume [9]. Pixels within the same voxel were averaged. The reconstruction was performed to obtain an isotropic voxel size of 0.2 mm.

F. MRI – 3D US image Fusion

The obtained ultrasound volume was fused with the MRI volume using marker-based rigid registration. For the registration, we used 4 lesions visible in the volume. The 5th lesion was used to measure the registration accuracy. The accuracy was defined as an average of distances between the remaining lesion within 3D US and MRI data after registration. The measurement was repeated for 5 combinations of the lesions and the average accuracy was measured. The lesions were segmented manually in both 3D US and MRI data utilizing 3D Slicer 4.10.2 [10].

G. Quantitative Analysis

To quantify the image quality, we measured the signal-to noise ratio (SNR) and the contrast-to-noise ratio (CNR) of the lesions using equations 2 and 3:

$$CNR = 20log_{10}\frac{|\mu_l - \mu_b|}{\sqrt{0.5(\sigma_l{}^2 + \sigma_b{}^2)}} \quad (2)$$

$$SNR = 20log_{10}\frac{\mu_l}{\sigma_l}, \quad (3)$$

where μ_l and σ_l are the mean value standard deviation of the gray level values within the lesion's volume, μ_b and σ_b are the mean value and standard deviation of the gray level values corresponding to the background. The background region was segmented at the same depth as the lesion.
Next, the measured SNR and CNR were compared to the reference values, calculated from the pre-processed B-mode images as described by in [11].

III. Results

A. Reconstruction

The reconstructed 3D ultrasound volume measured 77 x 77 x 69 mm^3, see figure 3. Only 24% of the data were obtained by interpolation. Only 5 out of 8 lesions were captured by the US (-22 dB, -5 dB, -4 dB, 3 dB, 7dB).

B. MRI – 3D US image Fusion

The result of the MRI – 3D US image fusion is shown in the fig. 4. The average accuracy for 5 measurements was 3.4 mm.

C. Quantitative Evaluation

The plotted data are presented in fig. 5. On average, the CNR and SNR were 24% and 6% higher comparing to the reference.

IV. Discussion

In this paper we present and evaluate quantitatively a novel automated robot-assisted volumetric breast US system. The average measured registration accuracy between MRI and acquired 3D US data was 3.4 mm. From fig. 4, it is clear that the two volumes correspond to each other and show similar features. Hence, the presented scanning approach facilitates MRI- 3D US fusion. This feature is important for biopsy planning and navigation in MURAB. The registration accuracy can be further improved by utilizing a larger number of internal markers. However, the slight mismatch between MRI and 3D US can also be caused by deformation of the phantom due to the scanning procedure with the US transducer. Solving this problem requires integration of a high precision pressure sensors as a feedback loop to minimize deformation during the US scanning.
The SNR and CNR are close to the reference which means that the internal structure of the phantom was not disturbed during the scanning process. However, the CNR and SNR were higher for the data, acquired with the described setup. An integral part of the volume reconstruction is averaging which decreases the noise level and thus increases the SNR and CNR values. During

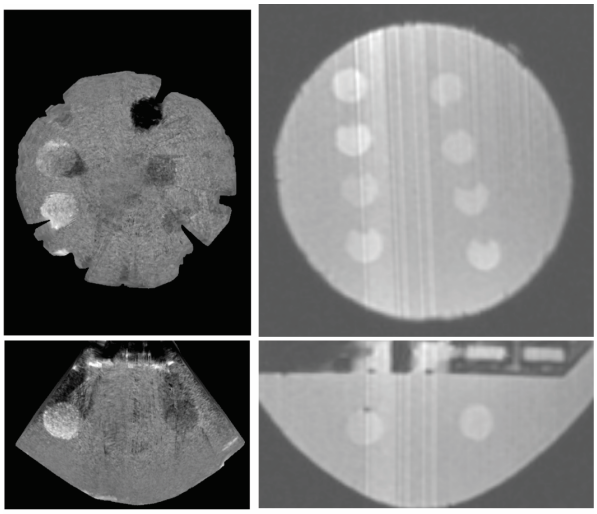

(a) (b)

Fig. 4. Correspondent cross section in coronal (top) and sagittal (bottom) directions between (left) 3D US and (right)MRI data after co-registration.

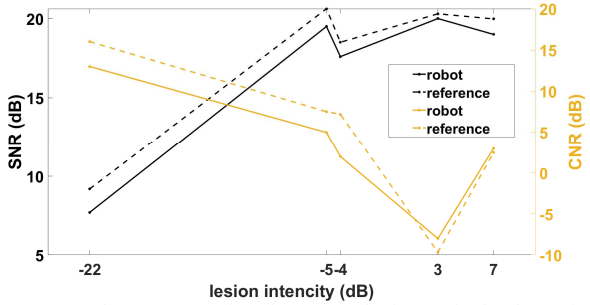

Fig. 5. SNR and CNR comparison between robotic acquired volumetric and reference US data.

the reconstruction also some artifacts are introduced which can be observed as inhomogeneities in fig. 4. Those are caused primarily by abovementioned deformation of the QBP and the stochastic nature of the time delay between image and spatial frames. This problem can be solved by introducing a triggering mechanism, precisely synchronizing both acquisitions.

In the presented experiment, the entire volume was not covered. Only 5 out of 8 lesions were fully captured. Imaging the full volume can be achieved by finding an optimal trajectory around the QBP/breast, taking into consideration the transducer geometry and contact area.

After improvements, the system requires further evaluation, first on soft phantoms and, next, *in vivo*.

V. Conclusion

Quantitative evaluation of the accuracy and image quality of the ultrasound data demonstrates that the presented scanning approach enables breast 3D US imaging, which facilitates MRI – 3D US image fusion. Despite the system requires technical improvements, to our believe, it can to become a new screening modality as well as a new alternative approach for breast biopsy.

Acknowledgment

This study has received funding by the European Union's Horizon 2020 research and innovation program under grant agreement no. 688188 as part of the MURAB project.

References

[1] J. Ferlay *et al.*, "Cancer incidence and mortality patterns in Europe: Estimates for 40 countries and 25 major cancers in 2018," *Eur J Cancer,* vol. 103, pp. 356-387, Nov 2018.

[2] M. Rahimzadeh, A. R. Baghestani, M. R. Gohari, and M. A. Pourhoseingholi, "Estimation of the cure rate in Iranian breast cancer patients," *Asian Pac J Cancer Prev,* vol. 15, no. 12, pp. 4839-42, 2014.

[3] G. Schueller, C. Schueller-Weidekamm, and T. H. Helbich, "Accuracy of ultrasound-guided, large-core needle breast biopsy," *Eur Radiol,* vol. 18, no. 9, pp. 1761-73, Sep 2008.

[4] M. Z. Mahmoud, M. Aslam, M. Alsaadi, M. A. Fagiri, and B. Alonazi, "Evolution of Robot-assisted ultrasound-guided breast biopsy systems," *Journal of Radiation Research and Applied Sciences,* vol. 11, no. 1, pp. 89-97, 2018/01/01/ 2018.

[5] "MRI and US Robotic Assisted Biopsy (MURAB)," 24.08.2020.

[6] M. K. Welleweerd, F. J. Siepel, V. Groenhuis, J. Veltman, and S. Stramigioli, "Design of an end-effector for robot-assisted ultrasound-guided breast biopsies," *International Journal of Computer Assisted Radiology and Surgery,* vol. 15, no. 4, pp. 681-690, 2020/04/01 2020.

[7] N. Anton, H. G. H. Hendrik, and L. d. K. Chris, "Real-time volumetric ultrasound imaging using free hand scanning," in *Proc.SPIE*, 2018, vol. 10580.

[8] P.-W. Hsu, R. W. Prager, A. H. Gee, and G. M. Treece, "Freehand 3D Ultrasound Calibration: A Review," in *Advanced Imaging in Biology and Medicine: Technology, Software Environments, Applications*, C. W. Sensen and B. Hallgrímsson, Eds. Berlin, Heidelberg: Springer Berlin Heidelberg, 2009, pp. 47-84.

[9] O. V. Solberg, F. Lindseth, H. Torp, R. E. Blake, and T. A. Nagelhus Hernes, "Freehand 3D ultrasound reconstruction algorithms--a review," *Ultrasound Med Biol,* vol. 33, no. 7, pp. 991-1009, Jul 2007.

[10] R. Kikinis, S. D. Pieper, and K. G. Vosburgh, "3D Slicer: A Platform for Subject-Specific Image Analysis, Visualization, and Clinical Support," in *Intraoperative Imaging and Image-Guided Therapy*, F. A. Jolesz, Ed. New York, NY: Springer New York, 2014, pp. 277-289.

[11] J. M. Thijssen, C. L. Weijers G Fau - de Korte, and C. L. de Korte, "Objective performance testing and quality assurance of medical ultrasound equipment," (in eng), no. 0301-5629 (Print).